

## Oscillation results from T2K

Patrick de Perio for the T2K Collaboration

*Department of Physics, University of Toronto, 60 St. George Street, Toronto M5S 1A7, Canada*

The T2K collaboration has combined the  $\nu_\mu$  disappearance and  $\nu_e$  appearance data in a three-flavor neutrino oscillation analysis. A Markov chain Monte Carlo (MCMC) results in estimates of the oscillation parameters and 1D 68% Bayesian credible intervals (CI) at  $\delta_{CP} = 0$  as follows:  $\sin^2 \theta_{23} = 0.520_{-0.050}^{+0.045}$ ,  $\sin^2 \theta_{13} = 0.0454_{-0.014}^{+0.011}$  and  $|\Delta m_{32}^2| = 2.57 \pm 0.11$ , with the point of highest posterior probability in the inverted hierarchy. Recent measurements of  $\theta_{13}$  from reactor neutrino experiments are combined with the T2K data resulting in the following estimates:  $\sin^2 \theta_{23} = 0.528_{-0.038}^{+0.055}$ ,  $\sin^2 \theta_{13} = 0.0250 \pm 0.0026$  and  $|\Delta m_{32}^2| = 2.51 \pm 0.11$ , with the point of highest posterior probability in the normal hierarchy. Furthermore, the data exclude values of  $\delta_{CP}$  between  $0.14\pi$ – $0.87\pi$  with 90% probability.

### 1 Neutrino Oscillations

The standard three neutrino model relates the flavor states of neutrinos to the mass states through the PMNS mixing matrix [1, 2]. This matrix is parameterized by three mixing angles ( $\theta_{12}$ ,  $\theta_{13}$ ,  $\theta_{23}$ ) and one CP violating phase ( $\delta_{CP}$ ). The flavor transition probabilities depend on these parameters as well as mass-squared splittings ( $\Delta m_{ij}^2$ ) and the mass hierarchy (MH), where  $\Delta m_{31}^2 > 0$  is defined as the normal hierarchy (NH) and  $\Delta m_{31}^2 < 0$  the inverted hierarchy (IH). All the parameters except  $\delta_{CP}$ , the  $\theta_{23}$  octant (maximal or non-maximal) and the MH have been previously measured as summarized in Reference [3].

The T2K experiment [4] aims to measure  $\theta_{23}$  and  $|\Delta m_{31}^2| \approx |\Delta m_{32}^2|$  precisely via  $\nu_\mu$  disappearance, with the survival probability given by

$$P_{\nu_\mu \rightarrow \nu_\mu} \approx 1 - (\cos^4 \theta_{13} \sin^2 2\theta_{23} + \sin^2 2\theta_{13} \sin^2 \theta_{23}) \sin^2 \Delta, \quad (1)$$

where  $\Delta = \Delta m_{31}^2 L / (4E)$ , and  $L$  and  $E$  are the neutrino flight length and energy, respectively. T2K also measures  $\nu_\mu$  to  $\nu_e$  appearance with the probability expanded in  $\alpha = \Delta m_{21}^2 / \Delta m_{31}^2$  as [5]

$$P_{\nu_\mu \rightarrow \nu_e} \approx \sin^2 2\theta_{13} T_1 - \alpha \sin 2\theta_{13} T_2 + \alpha \sin 2\theta_{13} T_3 + \mathcal{O}(\alpha^2), \quad (2)$$

where

$$T_1 = \sin^2 \theta_{23} \frac{\sin^2[(1-x)\Delta]}{(1-x)^2}, \quad (3)$$

$$T_2 = \sin \delta \sin 2\theta_{12} \sin 2\theta_{23} \sin \Delta \frac{\sin(x\Delta)}{x} \frac{\sin[(1-x)\Delta]}{(1-x)}, \quad (4)$$

$$T_3 = \cos \delta \sin 2\theta_{12} \sin 2\theta_{23} \cos \Delta \frac{\sin(x\Delta)}{x} \frac{\sin[(1-x)\Delta]}{(1-x)}, \quad (5)$$

and  $x$  is the correction due to the matter effect, which is positive (negative) for the NH (IH). Thus, T2K is sensitive to  $\theta_{13}$  and can explore  $\delta_{CP}$ , especially through the CP-odd term,  $T_2$ .

Since there are common parameters in Equations 1 and 2, a combined analysis of the  $\nu_\mu$  disappearance and  $\nu_e$  appearance samples rather than two separate analyses [6, 7] can improve the oscillation parameter measurements, in principle.

## 2 The T2K Experiment

An intense and high purity  $\nu_\mu$  beam is produced at J-PARC by colliding a 30 GeV proton beam with a graphite target, then focusing the resulting charged hadrons by magnetic horns prior to decay into neutrinos. The far detector, Super-Kamiokande (SK), is situated  $2.5^\circ$  off-axis from the neutrino beam resulting in a narrow-band energy spectrum peaked at 0.6 GeV, which maximizes the  $\nu_e$  appearance probability at a baseline of  $L = 295$  km and minimizes high energy backgrounds. This baseline corresponds to a matter effect correction of  $|x| \approx 5\%$ . The near detector complex, 280 m from the average neutrino production point, consists of an on-axis (INGRID) and off-axis (ND280) detector to constrain the beam direction, and neutrino flux and cross sections (xsec.), respectively.

The flux prediction is based on simulations tuned and constrained by hadron production data from the NA61/SHINE experiment and in-situ proton beam monitoring. The NEUT simulation package is used for the neutrino interaction model, with prior constraints based on external neutrino, pion and nucleon scattering cross section measurements.

The SK analysis uses a single-ring sample, which enhances charged current (CC) quasi-elastic (QE) events, separated into  $\mu$ -like ( $\nu_\mu$ ) and  $e$ -like ( $\nu_e$ ) sub-samples. The ND280 analysis selects charged current (CC)  $\nu_\mu$  interactions and separates the sample based on the number of reconstructed pions and decay electrons: CC0 $\pi$ , CC1 $\pi$  and CC Other. These topologies provide a strong constraint on the flux and interaction model governing CCQE scattering and resonant pion production, the signal and main background to the SK analysis, respectively. The reduction in the uncertainty on the SK predicted event rates due to the ND280 data is shown in Table 1. The SK and ND280 detector errors are constrained by calibration data and control samples such as cosmic rays and atmospheric neutrinos. More details of the SK and ND280 analyses can be found in previous T2K publications e.g. [6, 7] and the references therein.

Table 1: Summary of the effect of the systematic errors on the SK  $\nu_e$  and  $\nu_\mu$  candidate total event rates. The prior uncertainties in () brackets do not include the ND280 data.

Systematic Error Source	Relative Uncertainty (%)	
	$\nu_\mu$ Candidates	$\nu_e$ Candidates
Flux & Xsec. ND280 Constrained (Prior)	2.7 (21.7)	3.1 (26.0)
Xsec. ND280 Independent	5.0	4.7
Pion Hadronic Interactions	3.5	2.3
SK Detector	3.6	2.9
Total ND280 Constrained (Prior)	7.6 (23.4)	6.8 (26.8)

## 3 Oscillation Analysis

The likelihood function  $\mathcal{L}$  for the T2K oscillation analysis is given by

$$\begin{aligned} \mathcal{L}(\mathbf{o}, \mathbf{b}, \mathbf{x}, \mathbf{d}_{\text{ND}}, \mathbf{d}_{\text{SK}} | \mathbf{M}_{\text{ND280}}, \mathbf{M}_{\text{T2K-SK}}) = \\ P(\mathbf{M}_{\text{ND280}} | \mathbf{b}, \mathbf{x}, \mathbf{d}_{\text{ND}}) \times P(\mathbf{M}_{\text{T2K-SK}} | \mathbf{o}, \mathbf{b}, \mathbf{x}, \mathbf{d}_{\text{SK}}) \\ \times \pi(\mathbf{o}) \times \pi(\mathbf{b}) \times \pi(\mathbf{x}) \times \pi(\mathbf{d}_{\text{ND}}) \times \pi(\mathbf{d}_{\text{SK}}), \end{aligned} \quad (6)$$

where  $\mathbf{o}$ ,  $\mathbf{b}$ ,  $\mathbf{x}$ ,  $\mathbf{d}_{\text{ND}}$  and  $\mathbf{d}_{\text{SK}}$  are the neutrino oscillation, flux, cross section, ND280 detector and SK detector model parameters, respectively. The prior constraints,  $\pi$ , for the systematic (nuisance) parameters are described in Section 2 and typically assume multi-dimensional Gaussians, including correlations. For the oscillation parameters  $|\Delta m_{32}^2|$ ,  $\sin^2 \theta_{23}$ ,  $\sin^2 \theta_{13}$  and  $\delta_{CP}$ , a flat prior is assumed. Prior constraints from solar and reactor neutrino experiments [3] are also used, in particular  $\sin^2 2\theta_{13} = 0.095 \pm 0.01$ , which are assumed to be Gaussian. The prior

probability for the MH (sign of  $\Delta m_{32}^2$ ) is 0.5 for NH and IH, except where otherwise noted. The conditional probabilities,  $P$ , are assumed to be Poissonian and depend on the data and model predictions for each kinematic bin in each sample as follows. The ND280 samples,  $\mathbf{M}_{ND280}$ , are binned in two kinematic variables (2D), muon momentum and angle relative to the beam, as shown in Figures 1 and 2 for projections onto each variable. The SK samples,  $\mathbf{M}_{T2K-SK}$ , are binned in reconstructed neutrino energy assuming a CCQE interaction as shown in Figure 3. The data set used corresponds to  $0.657 \times 10^{21}$  protons on target (POT). Oscillation and systematic parameters are varied simultaneously across all samples when calculating the likelihood.

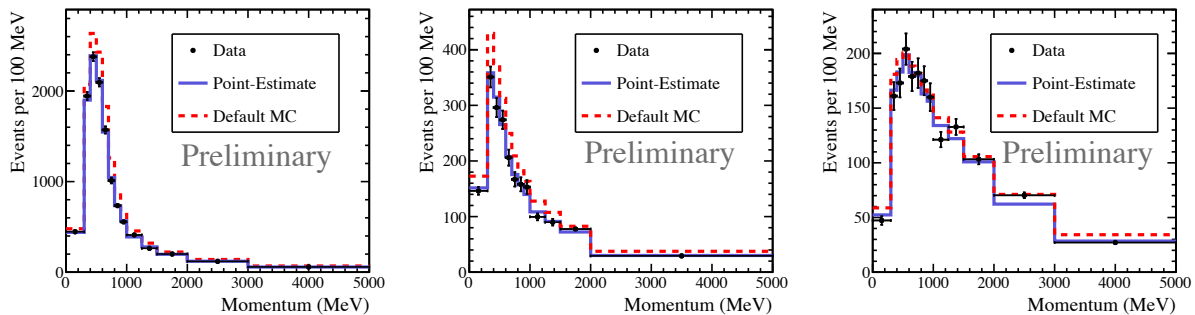


Figure 1 – The ND280 CC0 $\pi$  (left), CC1 $\pi$  (middle) and CC Other (right) event rates projected onto muon momentum for data, the default MC and point-estimates.

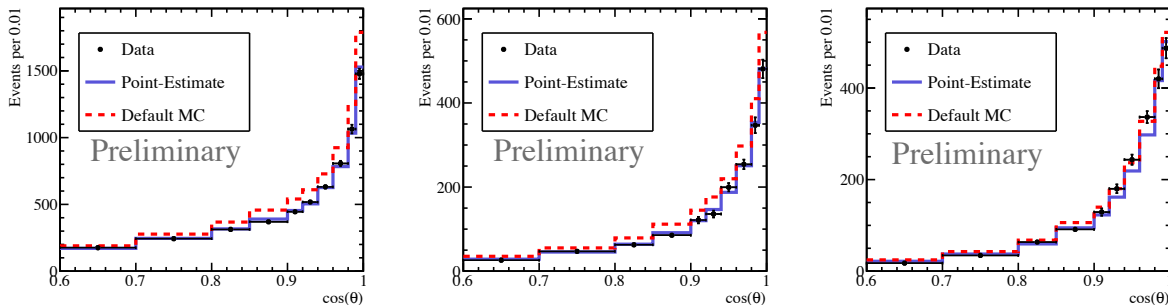


Figure 2 – The ND280 CC0 $\pi$  (left), CC1 $\pi$  (middle) and CC Other (right) event rates projected onto  $\cos \theta$  (muon angle relative to the beam) for data, the default MC and point-estimates.

A Bayesian analysis is performed using an MCMC to sample the likelihood in Equation 6 and marginalize over the nuisance parameters, producing posterior probability distributions for the oscillation parameters of interest. This differs from the previous T2K  $\nu_e$  appearance [6] and  $\nu_\mu$  disappearance [7] analyses that use frequentist-based methods such as minimization, profile-likelihoods and Feldman-Cousins contour construction. Another difference is the simultaneous inclusion of ND280 and SK data in Equation 6, where the previous analyses first fit the ND280 data only, then propagate the resulting parameter constraints to the SK fit under a Gaussian assumption. This assumption is not necessary in a simultaneous near and far analysis where any non-Gaussianities are preserved in the posterior probability distributions. There are some non-Gaussian systematics due to, for example, nuclear model uncertainties, however the difference between methods in the oscillation parameter estimates is currently negligible.

A posterior probability distribution for some parameter(s) of interest  $\mathbf{p}$  is constructed by marginalizing over the nuisance parameters  $\mathbf{f}$ , i.e. by integrating Equation 6:

$$\mathcal{L}_M(\mathbf{p}|\mathbf{M}) = \int P(\mathbf{M}|\mathbf{p}, \mathbf{f}) \times \pi(\mathbf{f}) d\mathbf{f}. \quad (7)$$

In practice, this is projecting all the steps of the MCMC onto the parameter(s) of interest, which can be model parameters or derived quantities. A *point-estimate*, in contrast to the *best-fit* from a minimization analysis, of  $\mathbf{p}$  is determined from the mode (most probable value) of the

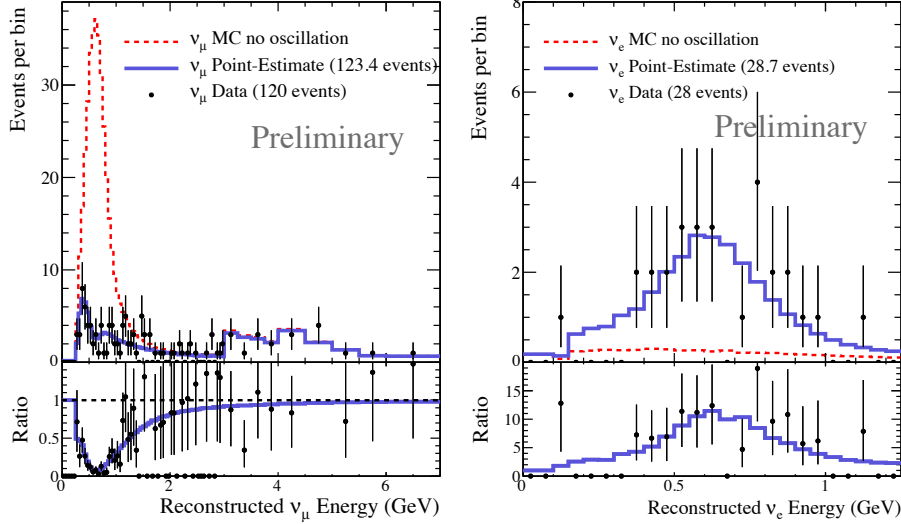


Figure 3 – The point-estimates (using T2K data only) and non-oscillated MC for the SK  $\nu_\mu$  (left) and  $\nu_e$  (right) event rates compared to data. The total integrated numbers of events are shown in () brackets. The ratios are the point-estimate over the no oscillation spectrum.

$\mathcal{L}_M(\mathbf{p}|\mathbf{M})$  distribution. Figures 1 to 3 show the point-estimates for each kinematic bin in each sample (derived quantities) compared to the data and the default predictions prior to inclusion of the data.

A 2D  $X\%$  *credible region* (CR) is defined as the region wherein the true parameter values lie with  $X\%$  probability, marginalized over all the other parameters. It is calculated by projecting the MCMC steps onto two parameters of interest  $\mathbf{p}$ , as in Equation 7, then finding the region such that

$$X = \iint_{\text{CR}} \mathcal{L}_M(\mathbf{p}|\mathbf{M}) d\mathbf{p}, \quad (8)$$

where  $\mathcal{L}_M$  is normalized to unity. The 68% and 90% CRs are shown for the  $\Delta m_{32}^2$ - $\sin^2 \theta_{23}$  and  $\delta_{CP}$ - $\sin^2 \theta_{13}$  parameter spaces in Figure 4 for the two cases of with and without the reactor constraint. The point-estimates in 4D ( $\sin^2 \theta_{13}$ ,  $\sin^2 \theta_{23}$ ,  $\Delta m_{32}^2$ ,  $\delta_{CP}$ ) are also shown and summarized in Table 2, where the 1D credible intervals (CIs) are evaluated as in Equation 8 except for one parameter only. The point-estimate line for  $\delta_{CP}$ - $\sin^2 \theta_{13}$  without the reactor constraint is determined by scanning  $\delta_{CP}$ , finding the mode in 3D then interpolating those points.

Table 2: The 4D point-estimates and 1D 68% CIs of each oscillation parameter with and without the reactor constraint. The CIs are calculated assuming the preferred MH, i.e. with prior probability  $\pi(\text{IH}) = 1$  or  $\pi(\text{NH}) = 1$ . The probabilities for the preferred MHs are shown in Table 4. The exclusion region for  $\delta_{CP}$  is shown in Figure 6.

	Pref. MH	$ \Delta m_{32}^2  [\times 10^{-3} \text{ eV}^2]$	$\sin^2 \theta_{23}$	$\sin^2 \theta_{13}$	$\delta_{CP}$
T2K-only	IH	$2.57 \pm 0.11$	$0.520^{+0.045}_{-0.050}$	$0.0454^{+0.011}_{-0.014}$	0 (fixed)
with reactor	NH	$2.51 \pm 0.11$	$0.528^{+0.055}_{-0.038}$	$0.0250 \pm 0.0026$	-1.601

A frequentist-based analysis was also produced. The best-fits for the oscillation parameters after minimizing over all parameters is shown in Table 3 for the NH and IH assumptions. The errors are based on the 1D constant- $\Delta\chi^2$  profile for each parameter. A comparison of the  $\Delta m_{32}^2$ - $\sin^2 \theta_{23}$  best-fits and 68% and 90% confidence level (CL) contours between the T2K, SK atmospheric [8] and MINOS [9] analyses is shown in Figure 5.

Allowed intervals for  $\delta_{CP}$  with the reactor constraint are shown in Figure 6 for the frequentist-based analysis including a Feldman-Cousins (FC) critical  $\Delta\chi^2$  correction ( $\Delta\chi_c^2$ ) and the Bayesian analysis using the posterior probability and CIs. Referring to Equation 2,  $\delta_{CP} \approx -\pi/2$  is preferred since the T2K data alone prefers a larger  $\theta_{13}$  compared to the reactor data.

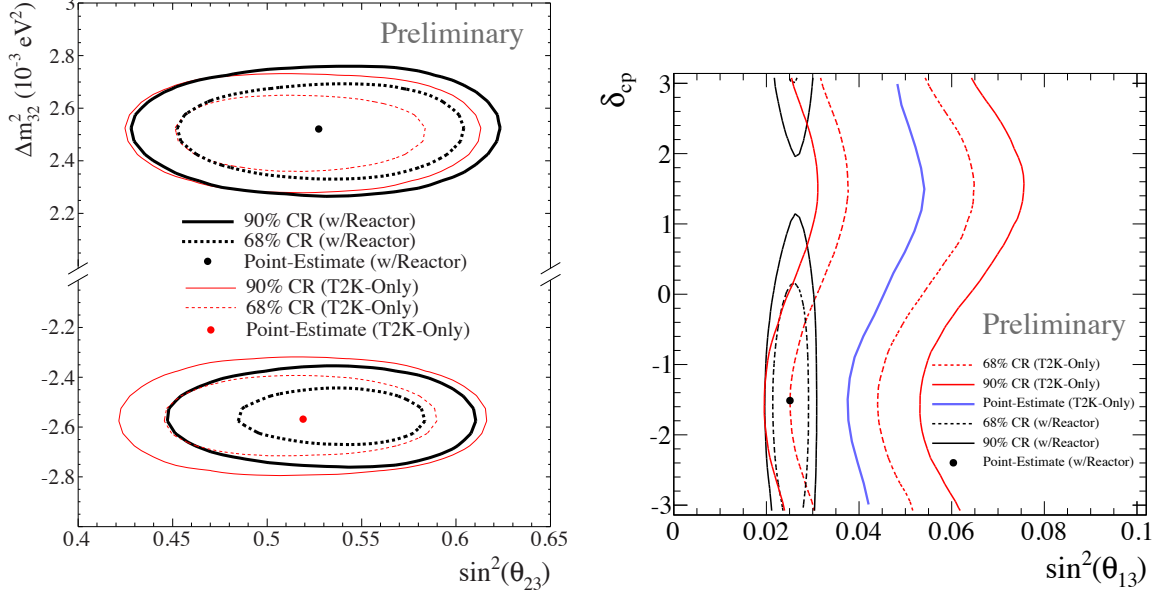


Figure 4 – The CRs in  $\Delta m_{32}^2$ - $\sin^2 \theta_{23}$  (left) and  $\delta_{CP}$ - $\sin^2 \theta_{13}$  (right) parameter spaces for T2K-only and reactor constrained analyses. The point-estimate for T2K-only in the left panel assumes  $\delta_{CP} = 0$ . Note the  $\Delta m_{32}^2$  axis includes the MH and so is not marginalized over the MH. Thus, the CRs also represent the probability of each MH, similar to the CL contours based on a global minimum in Figure 5.

Table 3: Best-fits and 1D constant- $\Delta\chi^2$  68% confidence intervals (errors) for the oscillation parameters assuming each MH with and without the reactor constraint.  $\Delta m_{32}^2$  ( $\Delta m_{13}^2$ ) is used for the NH (IH) assumption. The errors are not shown for  $\delta_{CP}$  in the T2K-only case since there is no strong constraint. The errors for the other parameters in the reactor-constrained case are not yet calculated and will be shown in a future publication, while the exclusion region for  $\delta_{CP}$  is shown in Figure 6.

	MH	$ \Delta m_{32,13}^2 $ [ $\times 10^{-3} \text{ eV}^2$ ]	$\sin^2 \theta_{23}$	$\sin^2 \theta_{13}$	$\delta_{CP}$ (rad)
T2K-only	NH	$2.51^{+0.11}_{-0.12}$	$0.524^{+0.057}_{-0.059}$	$0.0422^{+0.0128}_{-0.0212}$	1.9
	IH	$2.49 \pm 0.12$	$0.523^{+0.073}_{-0.065}$	$0.0491^{+0.0149}_{-0.0211}$	1.0
Reactor-constrained	NH	2.51	0.527	0.0248	-1.55
	IH	2.48	0.533	0.0252	-1.56

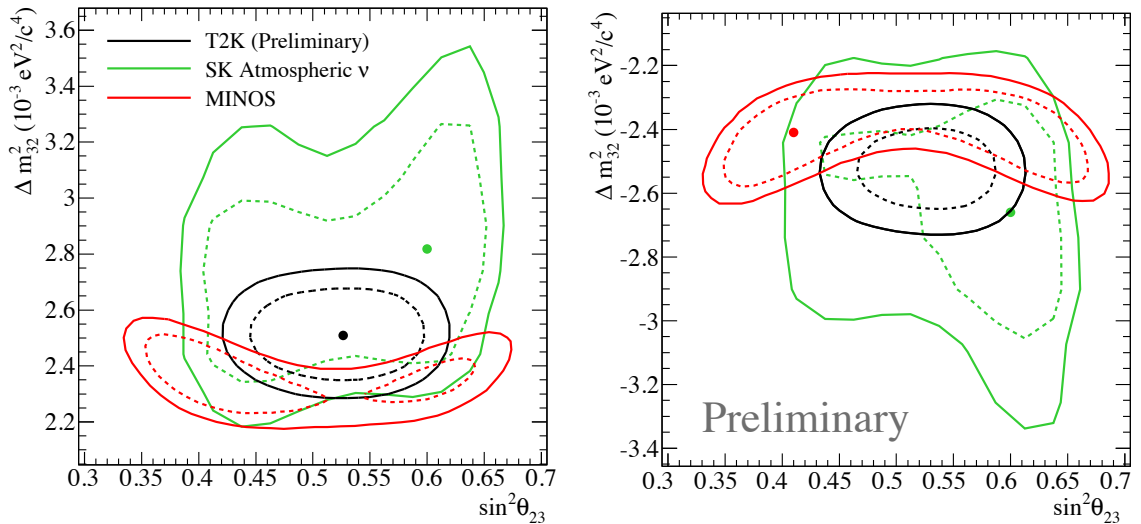


Figure 5 – The T2K best-fit point and constant- $\Delta\chi^2$  68% (dashed) and 90% (solid) CL contours in  $\Delta m_{32}^2$ - $\sin^2 \theta_{23}$  for NH (left) and IH (right) compared to those from the SK atmospheric [8] and MINOS [9] analyses. Note the T2K and MINOS analyses assume a global minimum across both MHs, while the SK analysis presents two independent fits.

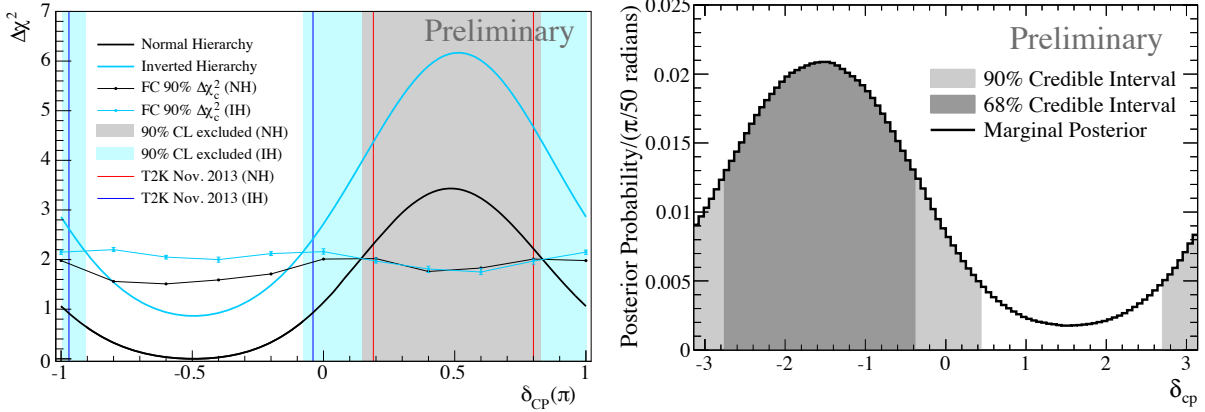


Figure 6 – Left: The  $\Delta\chi^2$  profile for  $\delta_{CP}$ , showing the 90% CL regions based on the FC  $\Delta\chi_c^2$  for NH and IH. The 90% CL inclusion is  $[-1.18, 0.15]\pi$  for NH and  $[-0.91, -0.08]\pi$  for IH. The vertical lines show the previous  $\nu_e$  appearance result [6]. Right: The posterior probability and 68% and 90% CIs for  $\delta_{CP}$ , marginalized over all the other parameters including the MH with priors  $\pi(\text{NH}) = \pi(\text{IH}) = 0.5$ . The 90% CI is  $[-1.11, 0.38]\pi$ .

The Bayesian analysis can also make interesting, though not yet significant, statements about the MH and  $\theta_{23}$  octant. Table 4 shows the posterior probabilities for each MH and  $\theta_{23}$  octant combination. The normal hierarchy and first octant is preferred when including the reactor constraint, similarly to the  $\delta_{CP}$  preference above. The MH,  $\theta_{23}$  octant and  $\delta_{CP}$  result here is in slight tension with the MINOS result [9].

Table 4: The posterior probability for each MH and  $\theta_{23}$  octant combination, assuming prior probabilities  $\pi(\text{NH}) = \pi(\text{IH}) = 0.5$  and  $\pi(\sin^2 \theta_{23} < 0.5) = \pi(\sin^2 \theta_{23} > 0.5) = 0.5$ . All other parameters are marginalized without (left) and with (right) the reactor constraint.

T2K-Only				Reactor-Constrained			
	NH	IH	Sum		NH	IH	Sum
$\sin^2 \theta_{23} \leq 0.5$	0.165	0.200	0.365	$\sin^2 \theta_{23} \leq 0.5$	0.179	0.078	0.257
$\sin^2 \theta_{23} > 0.5$	0.288	0.347	0.635	$\sin^2 \theta_{23} > 0.5$	0.505	0.238	0.743
Sum	0.453	0.547		Sum	0.684	0.316	

## 4 Conclusion and Outlook

The first T2K combined  $\nu_\mu$  disappearance and  $\nu_e$  appearance analyses based on  $0.657 \times 10^{21}$  POT is presented. T2K is producing the leading measurement on  $\theta_{23}$  and, combined with reactor neutrino data, non-trivial exclusion intervals in  $\delta_{CP}$ . The first anti-neutrino run is scheduled this year and, with increasing POT in the coming years, T2K will continue to lead the search for CP violation in the lepton sector.

## References

- [1] Z. Maki, M. Nakagawa, and S. Sakata, *Prog. Theor. Phys.* **28**, 870 (1962).
- [2] B. Pontecorvo, *Sov. Phys. JETP* **26**, 984 (1968).
- [3] Particle Data Group, *Phys. Rev. D* **86**, 010001 (2013).
- [4] T2K Collaboration, *Nucl. Instrum. Methods A* **659**, 106 (2011).
- [5] M. Freund, *Phys. Rev. D* **64**, 053003 (2001).
- [6] T2K Collaboration, *Phys. Rev. Lett.* **112**, 061802 (2014).
- [7] T2K Collaboration, *Phys. Rev. Lett.* **112**, 181801 (2014).
- [8] Super-Kamiokande Collaboration, arXiv:1310.6677 [hep-ex] (2013).
- [9] MINOS Collaboration, arXiv:1403.0867 [hep-ex] (2014).